論文 / 著書情報
Article / Book Information

Title	Corrosion of steels in lead bismuth flow
Author	Masatoshi KONDO, Minoru TAKAHASHI, Naoki SAWADA, Koji HATA
Citation	Journal of Nuclear Science and Technology, Vol. 43, No. 2, pp. 107-116
Issue date	2006, 2
Note	This is an Accepted Manuscript of an article published by Taylor & Francis in Journal of Nuclear Science and Technologyon 2006, 2 available online: http://www.tandfonline.com/10.1080/18811248.2006.9711073.

ORIGINAL PAPER

Corrosion of Steels in Lead-Bismuth Flow

Masatoshi KONDO[1], Minoru TAKAHASHI[2,*], Naoki SAWADA[2] and Koji HATA[3]

[1]*Department of Nuclear Engineering, Graduate School of Science and Engineering, Tokyo Institute of Technology*
N1-18, 2-12-1, O-okayama, Meguro-ku, Tokyo, 152-8550

[2] *Research Laboratory for Nuclear Reactor, Tokyo Institute of Technology*
N1-18, 2-12-1, O-okayama, Meguro-ku, Tokyo, 152-8550

[3]*Nuclear Development Corporation*
622-12 Funaishikawa, Tokaimura, Ibaraki 319-1111

(Received)

For the development of lead-bismuth cooled fast breeder reactors, the effect of Cr content in steels on corrosion resistance to high temperature lead bismuth was investigated by means of steel corrosion test performed in a flowing Pb-Bi for 1,000 hours. It was found that liquid metal corrosion was inhibited by single or multiple oxide layers formed on the steel surfaces. The oxide layers can be classified to an inner layer and an outer one. The existence of the inner oxide layer might be more important for the corrosion resistance since the inner one was compact and stuck to the steel surface while the outer one was easily broken into small pieces with cracks and peeled from the substrate. Stable Cr rich oxide layers were easily formed on the high Cr steels. The weight losses were lower in the steels with higher Cr contents. The content of Cr in the steel was effective to form the thin and compact Cr-rich oxide layer and suppressed the corrosion. In the case of Si rich steel, the weight loss was lower than the trends of weight loss with Cr content.

KEYWORDS: *corrosion, fast breeder reactor, liquid metal, lead bismuth, steel, oxide layer, chromium, oxide concentration*

I. Introduction

For the development of lead$_{45}$-bismuth$_{55}$ (Pb-Bi) cooled fast breeder reactors (FBRs)[1,2], one of the key issues is the compatibility of core and structural materials with Pb-Bi flow at high temperature [3].

The compatibility of steels in Pb-Bi is dominated by two types of corrosion [4], *i.e.* oxidation in Pb-Bi with high-oxygen concentration and so-called liquid metal corrosion (LMC) in Pb-Bi with low-oxygen concentration. Between these two types of corrosion, there exists an intermediate condition where steels are slightly oxidized, and the oxide layer protects substrate and consequently suppresses the LMC. Stability of the oxide layers depends on the properties and components of the oxide layers. The properties of the oxide layer influenced by the oxygen concentration in Pb-Bi [5,6] and the alloying elements of the substrate [7-10]. It has been expected that the content of chromium (Cr) in steels may promote the formation of stable oxide layer[7, 10]. However, the effect of Cr content on the steel corrosion in Pb-Bi has not been clarified experimentally, particularly by comparing various steels that have different Cr content.

In order to evaluate corrosion rate of the steels in Pb-Bi, the weight loss of specimens caused by the

dissolution of the alloying elements into Pb-Bi or detachment of unstable oxide layer during the exposure into Pb-Bi has been measured. For the measurement of the weight loss, it is necessary to remove adherent Pb-Bi to the specimens, although the oxide layers should not be removed for subsequent metallurgical analysis. However, in the previous experiment [11-12], adherent Pb-Bi was removed together with the oxide layers by immersing specimens in a hot sodium pool. It has been found that the immersion of the specimens in a hot glycerin pool is adequate for the removal of adhered Pb-Bi without removing the oxide layers[13]. Thus, in the present study, the adherent Pb-Bi was removed by using a hot glycerin pool for the measurement of weight loss.

The purpose of the present study is to investigate the effect of Cr content on corrosion characteristics and corrosion rates of steels in Pb-Bi flow experimentally for existing various steels which contained Cr between 1wt% and 18wt%. Particular purpose is to evaluate the relation between corrosion rate and the properties of the oxide layers formed on the steel surfaces.

II. Experimental apparatus and procedure

1. Pb-Bi forced convection loop

Figure 1 shows the schematic of the forced convective Pb-Bi circulation loop[14] used in the present corrosion test. The working fluid was Pb-Bi with a melting point of 125ºC. The loop consists of a high temperature region made of 9Cr steel and a low temperature region made of SS316 steel. The high temperature region has the electric heater, the corrosion test section and the oxygen sensor, and the low temperature region has the air cooler, the expansion tank, the electro-magnetic pump, and the electro-magnetic flow meter[15]. The cover gas of the expansion tank and the dump tank was argon having purity of 99.999%. Major specification of the loop is shown in **Table1.**

Pb-Bi in the dump tank was heated up to 180ºC and melted. The circulation loop was heated up to 180 ºC, and the Pb-Bi was charged from the dump tank into the circulation loop at a flow rate of approximately 0.5 l/min by the pressurizing the dump tank at 0.18 MPa with the loop pressure of 0.02 MPa. The Pb-Bi was circulated by the electro-magnetic pump at the rated operation flow rate, and the flow rate was measured by the electromagnetic flow meter. During the corrosion test, Pb-Bi was heated

by the electric heater to the temperature of 550 ºC at the inlet of the test section, and cooled down by the air cooler to the temperature of 400ºC at the outlet of the cooler. Due to the loop temperature difference, dissolved steel alloying elements in the hot region were transported to the low temperature region, and then precipitated there because of the lower solubility of the elements at the lower temperature. Therefore, a steady condition of dissolved element concentrations in the hot and cold regions were achieved without the saturation of the elements in the hot region[16].

Figure 2 shows schematics of rectangular plate-type steel specimens mounted in a cylindrical molybdenum specimen holder. The holder was wound by a Mo wire, and inserted into the test section as shown in **Fig.3**. Then, Pb-Bi flowed in two flow channels above and below the specimens which were 13 mm wide, 2 mm high and 425 mm long.

The oxygen concentration in Pb-Bi was measured with the oxygen sensor which was mounted at the outlet of the corrosion test section. The oxygen sensor was a solid electrolyte conductor made of a cylinder of magnesia stabilized zirconia (Zr_2O-MgO) with the reference fluid of oxygen-saturated

bismuth, that is, a mixture of 95wt%Bi and 5wt%Bi_2O_3. Electro-motive force between Pb-Bi and the reference fluid was measured and the oxygen potential in Pb-Bi was estimated from the Nernst equation.

2. Test material

Various steels were chosen as test material for the comparison of corrosion characteristics. Chemical components of test material are presented in **Table 2**. Low Cr steel, SCM420, is for structural material. Martensitic steel, F82H, has been developed as fusion blanket material [17]. STBA26 and NF616 is for boiler at high temperature. Martensitic steel, SUH3, has been developed for inner combustion material. Martensitic steel, ODS, has been developed as cladding material of fuel rods in sodium cooled fast breeder reactor[18, 19]. HCM12A and HCM12 [20] have been developed for the structural material of supercritical thermal power plant. Ferritic steel, SS405 and SS430, and austenitic steel, SS316, have been used as structural materials for chemical plant.

The sizes of the specimens are shown in Table 3. In order to remove the effect of surface roughness on corrosion behavior of each specimen when they were compared with each other[21], the surfaces were polished to be at the same smooth condition of arithmetical mean surface roughness Ra of 1.5μm The

polish is also needed to remove oxide layers as an initial surface condition.

The specimens were mounted in the specimen holder in the flow direction in the following order: (1) HCM12A, (2) SUH3, (3) STBA26, (4) NF616, (5) SS430, (6) SS405, (7) SS316, (8) F82H, (9) ODS, (10) SCM420. The steels mounted in upstream region were chosen to be more corrosion resistant based on the previous study[11] in order to prevent the influence of metal dissolution from specimens upstream on corrosion of specimens downstream.

3. Experimental conditions

Experimental conditions are summarized in **Table 4**. The specimens were exposed to Pb-Bi flow for 1,000 hours.

In order to form the protective oxide layer of Fe_3O_4 on steel surface that can suppress LMC, the oxygen potential in Pb-Bi was controlled to be slightly higher than Fe_3O_4 formation potential on the diagram of Gibbs free energy of oxide formation in **Fig. 4.** The corresponding oxygen concentration was above 10^{-8}wt%. According to the report of Fazio *et al.*[7], it is expected that an outer oxide layer of Fe_3O_4 and an inner layer of Fe $(Fe_{1-x}, Cr_x)_2 O_4$ might be formed for high Cr steels.

The electromotive force measured using the oxygen sensor at 550℃ was 0.43V during the operation. From the electromotive force, the oxygen concentration in Pb-Bi was calculated using the Nernst equation and oxygen solubility in Pb-Bi by Gromov *et al.*[16] as 3.7×10^{-8}wt% and 1.7×10^{-8}wt% using PbO and $Pb_{0.45}Bi_{0.55}O_{1.275}$ for ΔG^0, respectively. It is found in Fig.4 that the measured oxygen concentration was slightly higher than the Fe_3O_4 formation potential.

4. Procedure of specimen analysis

After the 1,000-hour exposure of the specimens to the Pb-Bi flow, the specimen holder was demounted from the test loop, and immersed in a glycerin pool at the temperature of 180℃ to remove adherent Pb-Bi from the outside and inside of the holder. Then, the holder was opened and the specimens were taken out of the holder, and rinsed again in glycerin pool at the temperature of 180℃ to melt and remove adherent Pb-Bi from the specimen surfaces without removal of the oxide layers. Finally, glycerin on the specimen surface was removed in warm water at the temperature of 70℃.

The surfaces of the specimens were observed before and after the exposure to inspect the occurrence of erosion. In order to determine the corrosion rate, weight losses of the specimens were measured using an electro reading balance with an accuracy of 0.1mg. The specimens were cut at the span wise center and the cross sections were polished, and then observed by a scanning electron microscope (SEM) and analyzed by an energy-dispersive X-ray spectrometer (EDX).

III. Experimental results

1. Surface observation

The surfaces of the specimens after the 1,000-hour exposure are shown in **Fig.5**. It can be seen that no appreciable traces of erosion existed on all of the steel surfaces. The surface state was similar to each other in all the specimens. The colors of the steel surfaces changed from initial metallic luster before the exposure into black after the exposure, which suggested the formation of corrosion products or oxide layers on the surfaces.

2. Weight loss

Figure 6 shows the measured weight losses of the specimens. All the steels lost their weight during the exposure. The weight loss in SCM420 was the largest among all the steels. The weight loss of F82H, ODS and HCM12A were also large. The weight losses of SUH3 and SS430 were less than the other steels. There were weight increases in HCM12, which could be also attributed to the formation of thick oxide layers.

The weight loss of SS316 was not able to evaluate in the present experiment. That was because Pb-Bi penetrated into the porous layer formed by the dissolution of Ni and Cr into Pb-Bi was not completely removed in the glycerin. The weight loss of F82H might be larger than the measured one since Pb-Bi that rarely penetrated into steel matrix could not be completely removed by glycerol.

3. Oxide layer

(1) HCM12A and HCM12

On the surfaces of HCM12A, triple oxide layers were formed as shown in **Fig.7 (a).** These layers can be classified into the outer layer A, the middle layer B and the inner layer C. The Fe-rich outer layer A was broken into some pieces and peeled from the substrate, while the Cr-rich middle and inner layers stuck to the substrate stably (Fig.7 (a) No.1, 2 and 3). The thickness of the each layer is shown in **Table5**.

It was observed in HCM12 (**Fig.7 (b)**) that triple oxide layer formation was similar to that in HCM12A. The outer layer A consisted of the small fragments. The middle layer B was compact and stuck to the substrate. The inner layer was merged with steel matrix as if it had no clear interface. The

weight ratio of Fe to Cr in the outer layer, middle layer and inner layer was app. 3:1, 2.1 and 7:2, respectively (Fig.7 (b) No1, 2 and 3). The major difference between the layers in HCM12A and HCM12 is that Cr enriched not only in the middle layer but also in the outer layer on the latter steel. In both of the steels, no sign of Pb-Bi penetration was observed beneath these layers.

(2) NF616 and STBA26

Triple oxide layer was observed on NF616 surface (**Fig.7 (c)**). There were some cracks in the outer layer where Fe was poor and Cr was slightly enriched compared with that of the matrix (Fig.7 (c) No.1). Fe content was poor and Cr and W were enriched in the middle layer (Fig.7 (c) No.2) which might be effective together with the quite thin oxide layer close to the surface of the inner layer to protect the steel from corrosion.

The surface of STBA26 was covered by the oxide layer with double layer structure: (**Fig. 7 (d)**). The outer layer A, where Cr was enriched (Fig.7 (d) No.1), seemed to correspond to the middle layer in

NF616 (Fig. 7 (c) No.2) since a developing scale could be observed on the layer A. The inner layer was very thin as it merged with the steel matrix.

(3) SS430 and SS405

Double oxide layer was observed on the surface of SS430 as shown in **Fig 7(e)**. The Cr-enriched outer layer had some cracks. Inner layer B consists of the small pieces.

On the SS405 surface (**Fig.7 (f)**), the app.6.7μm thick outer layer A and app.4μm thick inner layer B were observed. In the outer layer A, Cr was enriched (Fig.7 (f) No.1), and there were some cracks particularly on the rough part of the steel surface[21].

(4) ODS

It was observed in ODS that the oxide layers were formed and that composed of two layers: outer layer A of app.7μm in thickness and inner layer B of app.11μm in thickness (**Fig 7 (g)**). The Cr-enriched outer layer A was broken to small fragments and peeled from the inner layer B. In the thick inner layer which stuck to the matrix stably, Cr was enriched only slightly compared with that of the steel matrix

(Fig. 7 (g) No.2). Some transverse cracks existed on the convex part of the steel surfaces[22].

(5) F82H

Double oxide layer: app.8.3μm thick outer layer A and app.4μm thick inner layer B were observed (**Fig. 7 (h)**). The Cr-enriched outer layer A was peeled form the inner layer B. The W enriched inner layer was also peeled from the surface (Fig.7 (h) No. 2). Beneath the inner layer, Pb-Bi penetrated into the steel matrix.

(6) SS316

Single oxide layer was formed on the surface of SS316. Fe was poor and Cr was enriched in the layer (**Fig 7 (i) and (j)**). The Pb-Bi penetration was partially caused by the dissolution of Ni and Cr into Pb-Bi. However, the depth was app.15μm which was much shallower than that caused erosion without the formation of the oxide layer in previous study [11].

(7) SUH3

There were two layers on the surface of SUH3 as shown in **Fig.7 (k)**. The outer oxide layer was peeled from the steel surface. The inner layer was thin and the surface is smooth without damage. It has been found by EDX analysis that Si was enriched only in the inner layer.

(8) SCM420

Figure 7 (l) shows that SCM420 characterized by low-alloy steel has only single layer with cracks. In the layer, Cr was not enriched.

IV. Discussion

1. Effect of oxide layer formation on corrosion of steels in Pb-Bi

All the test steels formed the oxide layers in Pb-Bi flow. Although LMC occurred in F82H and SS316, the intensities of the LMC in F82H and SS316 were much weaker than those in the pervious results [11] where the oxide layers were not formed because of low oxygen content in Pb-Bi. Therefore, the formation of the oxide layers seemed to be effective to inhibit the LMC.

2. Effect of oxide layer structure on corrosion resistance

The structures of the oxide layers depended on the type of the steels as shown in Fig.7. Except for the single layers formed on SCM420 and SS316, the layers on the other steels could be observed as multiple which were composed of different chemical composition as the same as reported by some researchers[7-10,13].

As for the property of the multiple layers, the most of the outer layers were cracked and broken into some pieces. In other words, it is not be effective as barrier for the corrosion. On the contrary, the inner

one was compact and stuck to the steel surface. Similar phenomena were also reported in ref [13]. Thus, the formation of the compact inner layer might be more important to inhibit the LMC.

The formation mechanism of multiple oxide layers on the steels in Pb-Bi could be explained as follows. Fe-rich oxide layer as the outer layer was formed by the reaction of Fe and oxygen in Pb-Bi. Then, oxygen diffused from the Pb-Bi into the steel matrix across the outer layer and reacted chemically with Cr since the oxygen potential was lower than that in Pb-Bi flow due to the existence of the outer layer as barrier. This oxygen diffusion might produce a thin and stable oxide layer close to the surface of the steel matrix. Once the Cr-rich oxide layer was formed, Fe could not be dissolved easily into the Pb-Bi because of the barrier of the Cr-rich oxide layer.

3. Effect of alloying elements on oxidation corrosion in Pb-Bi

As suggested in ref [7], once the oxide layers were formed on the steel surfaces in Pb-Bi, the corrosion might change from the LMC to the oxidation corrosion.

It has been found in the oxidation corrosion of the steels in air or vapor at high temperature[21] that low

Cr content in the steels enhanced the formation of Fe rich oxide layer. Then, the low Cr steels caused the oxidation corrosion due to the break away of the unstable oxide layer. However, steels with high Cr content had the resistance for the oxidation corrosion due to the formation of the stable Cr rich oxide layers.

As the same as the case of the corrosion in air or vapor, high Cr steels like HCM12, HCM12A, SS405 and SS430 showed higher corrosion resistance than that in low Cr steels in Pb-Bi flow (**Fig.8**). The weight loss of the steels was lower as the Cr content was higher in the order of SCM420, STBA26, ODS, SS405 and SS430. The weight loss of SUH3 was remarkably lower than those of the other steels possibly due to the influence of the formation of stable and thin Si-rich oxide layer [9,10].

The thickness of the oxide layers was thinner in general as Cr contents were higher in the steels, which leads to stable protective layers. The steels which contained Cr above 12wt%: HCM12, HCM12A, SS405 and SS430 formed the oxide layers, in which Cr was enriched as the weight ratio of Fe to Cr were approximately 2:1, while the steels contained Cr below 12wt%: F82H, ODS, STBA26,

and NF616 formed the oxide layers, in which the weight ratio of Fe to Cr were approximately 4:1.

These facts indicated that the steels which had higher Cr contents form the more stable oxide layer, and consequently more corrosion resistant in the Pb-Bi flow.

In the case of W rich steels: HCM12A (1.94W), F82H (1.94W) and NF616 (1.8W), the content of W might play a particular role in the formation of the multiple oxide layers since W was enriched only in the inner layer. The inner layers had showed clear interface with the outer layer and the steel matrix.

The content of Si in SUH3 might be effective to form a thin and stable inner oxide layer.

V. Conclusion

Corrosion characteristics of the steels in liquid lead bismuth were investigated by means of the steel corrosion test performed in flowing lead bismuth. Conclusions are as follows:

1) The oxide layers were formed on all the test steels in flowing Pb-Bi at the oxygen potential higher than that required for the formation of Fe_3O_4.

2) Beneath the oxide layers, the trace of liquid metal corrosion was not observed except for austenitic steel SS316 and martensitic steel F82H.

3) The oxide layers had a multiple layer structure. The existence of the thin and compact inner oxide layer was important for the steels to be more corrosion resistant in Pb-Bi flow.

4) In the oxide layers which were formed on high Cr steels: HCM12, HCM12A, SS405, SS430, Cr was enriched.

5) The weight loss was lower in the steels with higher Cr content in general, although there was exception of austenitic steel, SS316 and Si rich steel, SUH3.

Acknowledgments

The authors thank Dr. A. Otsubo, Mr. T. Iguchi, Dr. Y. Qi, Prof. H. Sekimoto and Prof. Yano for their valuable discussion, and Mr. M. Imai, Dr. S. Yoshida, Mr. A. Yamada and Dr. S. Qiu for their experimental assistance. The authors acknowledge the supply of the test material F82H of Japan Atomic Energy Research Institute (JAERI) and Koukan Keisoku K.K., and the supply of the test material ODS of Japan Nuclear Cycle Development (JNC). This study was a part of the Project of Technical Development of Innovative Reactor System supported financially by the Ministry of Education, Culture, Sports, Science and Technology of Japan.

References

1) M.Takahashi, T.Obara, T.Iguchi, A.Otsubo, M.Kondo, Y.Qi, K.Hata, K.Hara, S.Uchida, H.Osada, Y.Kasahara, K.Matsuzawa, N.Sawa, Y.Yamada, K.Kurome and Y.Okubo, "*Design and Experimental Study for Development of Pb-Bi Cooled Direct Contact Boiling Water Small Fast Reactor (PBWFR)*", Proc. of Int. Conf. Nuc. Eng., Pittsburgh, USA, Jun. 13-17, 2004, Paper 4058 (2004)

2) S.Uchida, H. Osada, Y. Kasahara, M. Takahashi and K. Hata, "*A Feasibility Study on the Lead-bismuth Cooled Direct Contact Boiling Water Fast Reactor*", Proc. of 11th Int. Conf. Nuc. Eng., Tokyo, Japan, Apr. 20-23, ICONE11-36320 (2003).

3) M.Takahashi, M.Igashira, T.Obara, H.Sekimoto, K.Kikuchi, K.Aoto and T.Kitano, "*Studies on Materials for Heavy-Liquid-Metal-Cooled Reactors in Japan*", Proc. of 10th Int. Conf. Nuc. Eng., Arlington, Virginia, USA, Apr. 14-18, ICONE10-22166 (2002).

4) I.V.Gorynin, G.P.Karzov, V.G.Markov, V.S.Lavrukhin, V.A.Yakolev, "*STRUCTUAL MATERIALS*

FOR POWER PLANTS WITH HEAVY LIQUID METALS AS COOLANTS", Proc. of HLMC1999, 87-100

5) Ning Li, "*Active control of oxygen in molten lead-bismuth eutectic systems to prevent steel corrosion and coolant contamination*", J.Nuc.Mater. **300**, 73-81 (2002)

6) G..Muller, A.Heinzel, G.Schumacher, A.Weisenburger, "*Control of oxygen concentration in liquid lead-bismuth*", J.nuc.mater. **321**, 256-262 (2003)

7) C.Fazio, G.Benamati, C.Martini, G.Palombarini, "*Compatibility tests on steels in molten lead and lead-bismuth*", J.Nucl.Mater. **296**, 243-248 (2001)

8) G.Benamati, C. Fazio, H.Pinakova, A.Rusanov, "*Temperature effect on the corrosion mechanism of austenitic and martensitic steels in lead-bismuth*", J.Nucl.Mater. **301**, 23-27 (2002)

9) Ronald.G..Ballinger, J.Lim, Eric P. Loewen, "*The Effect of Silicon on the Corrosion of Iron on Lead bismuth Eutectic*", Proc. of 11th International Conf. Nucl. Eng., Tokyo, Japan, Apr. 20-23, ICONE11-36531 (2003).

10) J.Lim, R.G.Ballinger, and P.W.stable, "*Fe-Cr-Si Alloy Development for Pb-Bi Eutectic service*", Global 2003, New Orleans, 2100-2103

11) M. Takahashi, H. Sekimoto, K. Ishikawa, T. Suzuki, K. Hata, S. Qiu, S. Yoshida, T. Yano, and M. Imai, "*Experimental Study on Flow Technology and Steel Corrosion of Lead Bismuth*," *Proc. of 10th International Conf. Nucl. Eng.*, ICONE10-22226 (2002).

12) M.Takahashi, M.Kondo, N.Sawada and K.Hata, "*Corrosion of steels in Lead-Bismuth Flow*", Global 2003, New Orleans, 2104-2112

13) F. Barbier, A. Rusanov, "*Corrosion behavior of Steels in flowing lead-bismuth*", J. Nucl. Mater. 296 , 231-236 (2001)

14) M.Takahashi, N. Sawada, H. Sekimoto, M. Kotaka, T. Yano, S. Uchida, K. Hata, and T. Suzuki, "*Design and Construction of Lead-bismuth Corrosion Test Loop and Test Plan*," Proc. of 8th Int. Conf. Nucl. Eng., Baltimore, ICONE10-8507 (2000).

15) M.Kondo, M.Takahashi, A.Yamada, K.Ishikawa, N.Sawada and T.Suzuki, "*Metallurgical Study on*

Performance of Electro-Magnetic Flow meter for liquid lead-bismuth", *Proc. of 12th Int. Conf. Nucl. Eng.*, Baltimore, ICONE12-49218 (2004).

16) B.F.Gromov, Y.I.Orlov, P.N.Martynov, V.A.Gulevsky, *"The problems of technology of the heavy liquid metal coolants (Lead-bismuth, Lead)"*, Proc. of HLMC1999, 87-100

17) S.Jitsukawa, M.Tamura, B. van der Schaaf, R.L.Klueh, A.Alamo, C.Peterson, M.Schirra, P.Spaetig, G.R.Odette, A.A. Tavassoli, K.Shiba, A.Kohyama and A.Kimura, *"Development of an expensive database of mechanical and physical properties for reduced-activation martensitic steel F82H"*, J.Nucl.Mater. **307-311**, 179-186 (2002)

18) S.Ukai, M.Fujiwara, "*Prospective of ODS alloys application in nuclear environments*" J.Nucl.Mater. **307-311**, 749-757 (2002)

19) E.Yoshida, S.Kato, "Sodium compatibility of ODS steel at elevated temperature", J.Nuc.Mater xxx(2004)xxx-xxx, Article in press.

20) K.Rodak, A.Hernas, A.Kielbus, "Substructure stability of highly alloyed martensitic steels for

power industry", Nuc.chem.and phis.**81**, 483-485 (2003)

21) K.Sugimoto, *"Passivity-The trend of studies for Recent 20 years"*, Zairyo-to-Kankyo, 53,159-161, (2003)

22) M.Kondo, M.Takahashi, S.Yoshida, N.Sawada, *"Effect of Surface Roughness of Steels on Oxide Layer Formation in a Liquid Lead-Bismuth Flow"*, Proc. of Int. Cong. Advances in Nuclear Power Plants, Pittsburgh, USA, Jun. 13-17, Paper 4044 (2004)

Table captions

Table 1 Specifications of forced convective Pb-Bi circulation loop

Table 2 Chemical components of test steels

Table 3 Size of specimens

Table 4 Experimental conditions

Table 5 Thickness of oxide layers and Pb-Bi penetration obtained from SEM analysis

Figure captions

Fig. 1 Schematic diagram of corrosion test loop

Fig. 2 Specimen holder

Fig. 3 Test section

Fig. 4 Diagram of oxygen potential; symbol of black triangle: ΔG^0 is estimated from oxygen potential of $Pb_{0.45}Bi_{0.55}O_{1.275}$, symbol of black square: that is estimated from oxygen potential of PbO

Fig. 5 Appearance of specimen surfaces in Mo holder after 1,000 hr-exposure to Pb-Bi flow

Fig. 6 Weight losses of specimens during 1,000 hr-exposure to Pb-Bi flow of specimens

Fig. 7 Oxide layers and metal elements in following material after 1,000 hr-exposure to Pb-Bi flow

(a) HCM12A,

(b) HCM12,

(c) NF616,

(d) STBA26,

(e) SS430,

(f) SS405,

(g) ODS,

(h) F82H,

(i) SS316 (Content of Fe),

(j) SS316 (Content of Cr),

(k) SUH3

(l) SCM420

Fig. 8 Relation between weight losses and chromium content in steels

Table 1 Specifications of forced convective Pb-Bi corrosion test loop

Pb-Bi inventory in loop	0.022 m^3
Volume in dump tank	0.066 m^3
Maximum test temperature	823 K
Maximum system pressure	0.4 MPa
Maximum flow rate	6 l/min
Maximum velocity in test section	2 m/s
Heater and cooler power	22 kW
Structural material in hot region	9Cr-1Mo steel
Structural material in cold region	SS316

Table 2 Chemical components of test steels

	Cr	Mo	W	Si	others
SCM420	1.2	0.2	-	0.2	
F82H	7.7	1.94	1.94	0.1	0.01Ti-0.01Cu
NF616	9	0.5	1.8	0.3	
STBA26	9	1	-	0.2	
SUH3	11	1	-	2	0.4C
ODS	11.7	-	1.9	-	0.29Ti-0.23Y_2O_3-0.18Y
HCM12A	12	0.3	1.9	0.3	0.9Cu
HCM12	12.1	1.1	1.0	0.3	
SS405	12	-	-	1	0.1Al
SS316	18	2-3	-	0.1	10-14Ni
SS430	18	-	-	0.75	

Table3 Size of specimens

	Length	Width
HCM12A	30	15
HCM12	10	15
SUH3	30	15
STBA26	55	15
NF616	10	15
SS430	55	15
SS405	10	15
SS316	10	15
F82H	10	15
ODS	10	15
SCM420	(Spacer)	15

Table 4 Experimental conditions

Exposure time		1,000 hrs
Pb-Bi temperature in test section		550 ℃
Pb-Bi temperature in low temperature sections of loop		400 ℃
Pb-Bi velocity in test section		1 m/s
Pb-Bi flow rate		3 l/min
Oxygen concentration in Pb-Bi	ΔG^0 of PbO	3.7×10^{-8} wt%
	ΔG^0 of $Pb_{0.45}Bi_{0.55}O_{1.275}$	1.7×10^{-8} wt%

Table 5 Thickness of oxide layers and Pb-Bi penetration

obtained from SEM analysis

	Thickness (μm)			
	Outer layer	Middle layer	Inner layer	Pb-Bi penetration
SCM420	-	-	17	-
F82H	-	8.3	4	8.3
STBA26	-	10	2	-
NF616	3	5	2	-
SUH3	-	6.6	1	-
ODS	-	7	11	-
HCM12A	4	4	4	-
HCM12	3	8.2	5	-
SS405	-	6.7	3.3	-
SS316	-	-	4.1	8
SS430	-	6.7	4	-

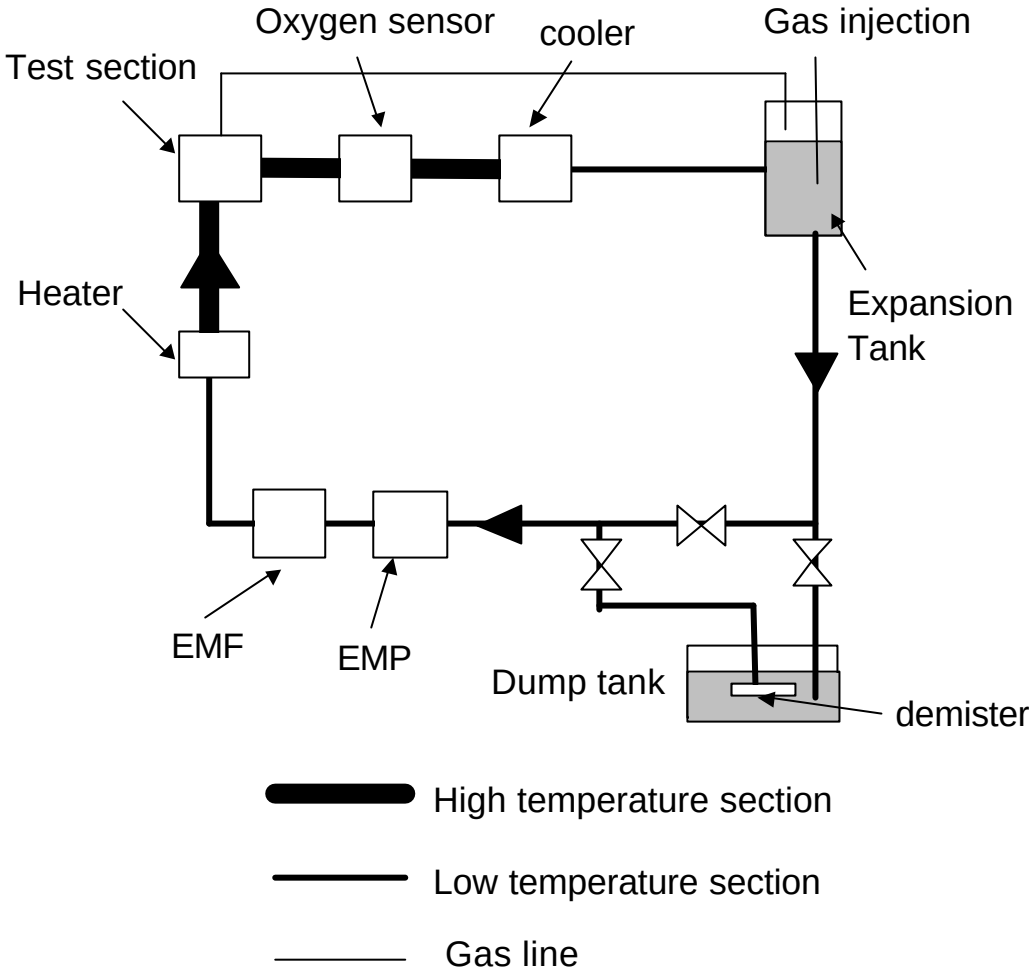

Fig. 1 Schematic diagram of corrosion test loop

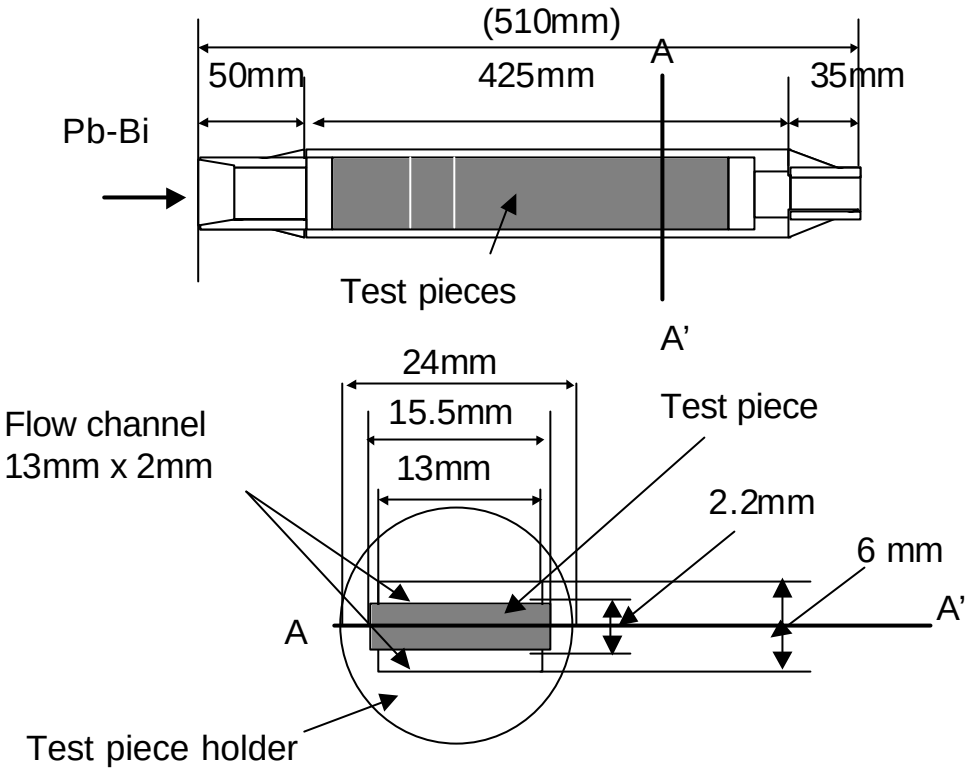

Fig. 2 Specimen holder

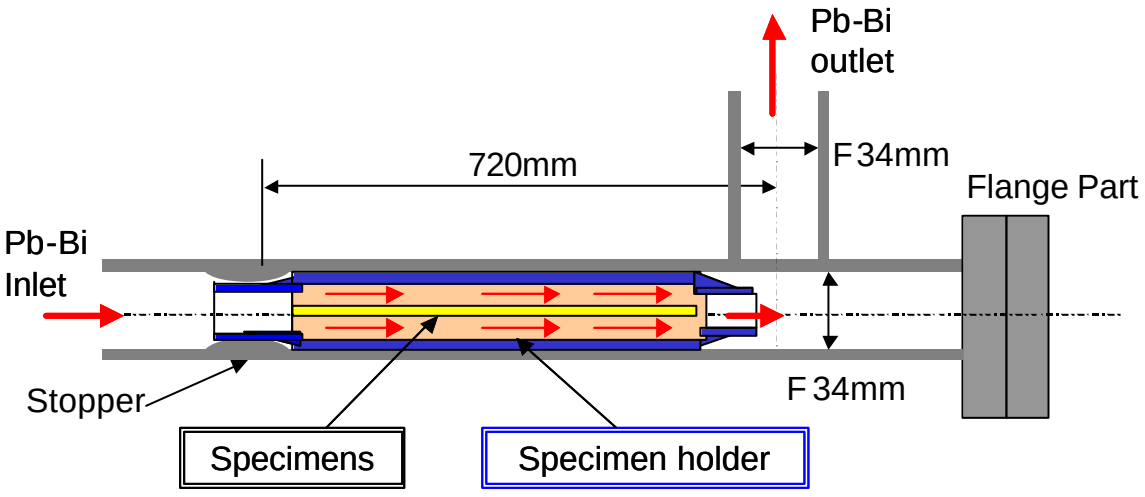

Fig. 3 Test section

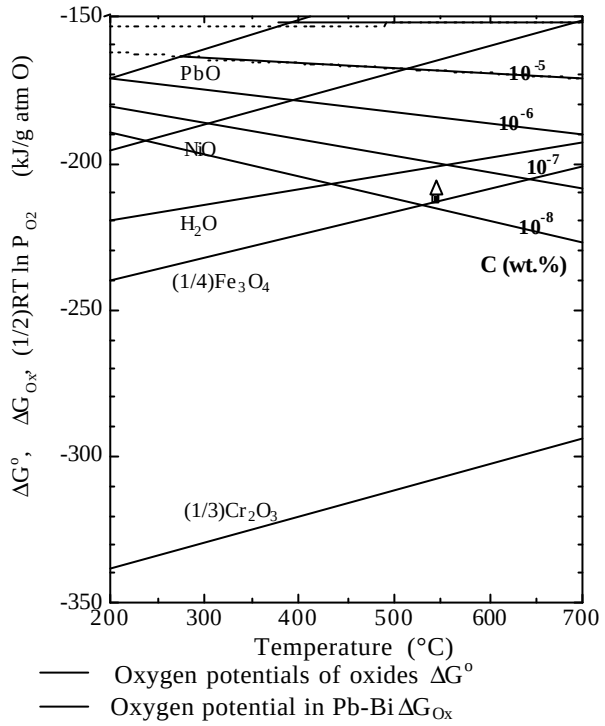

Fig. 4 Diagram of oxygen potential; symbol of black triangle: ΔG^0 in Eq.(2) is estimated from oxygen potential of $Pb_{0.45}Bi_{0.55}O_{1.275}$, symbol of black square: that is estimated from oxygen potential of PbO

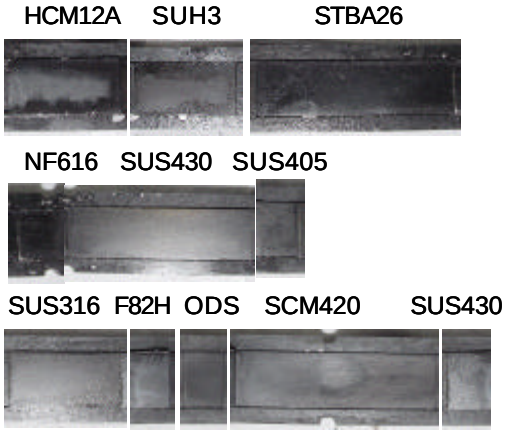

Fig. 5 Appearance of specimen surfaces in the Mo holder after 1,000 hr-exposure to the Pb-Bi flow

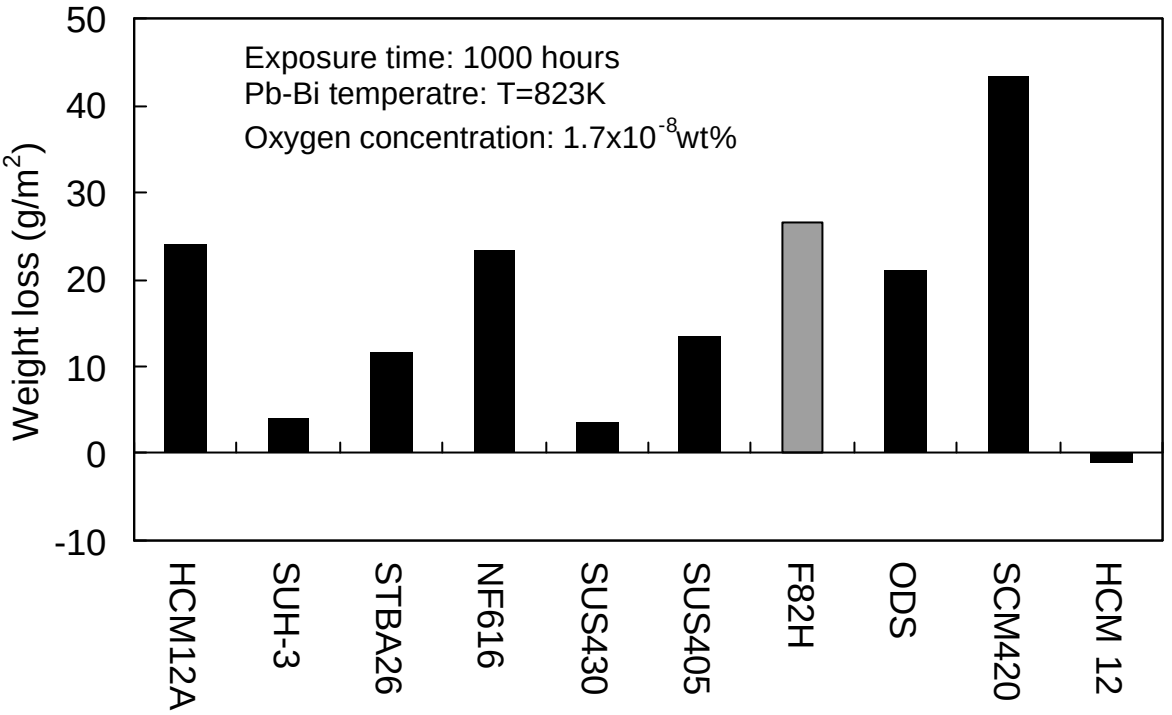

Fig. 6 Weight losses of specimens during 1,000 hr-exposure to the Pb-Bi flow of specimens

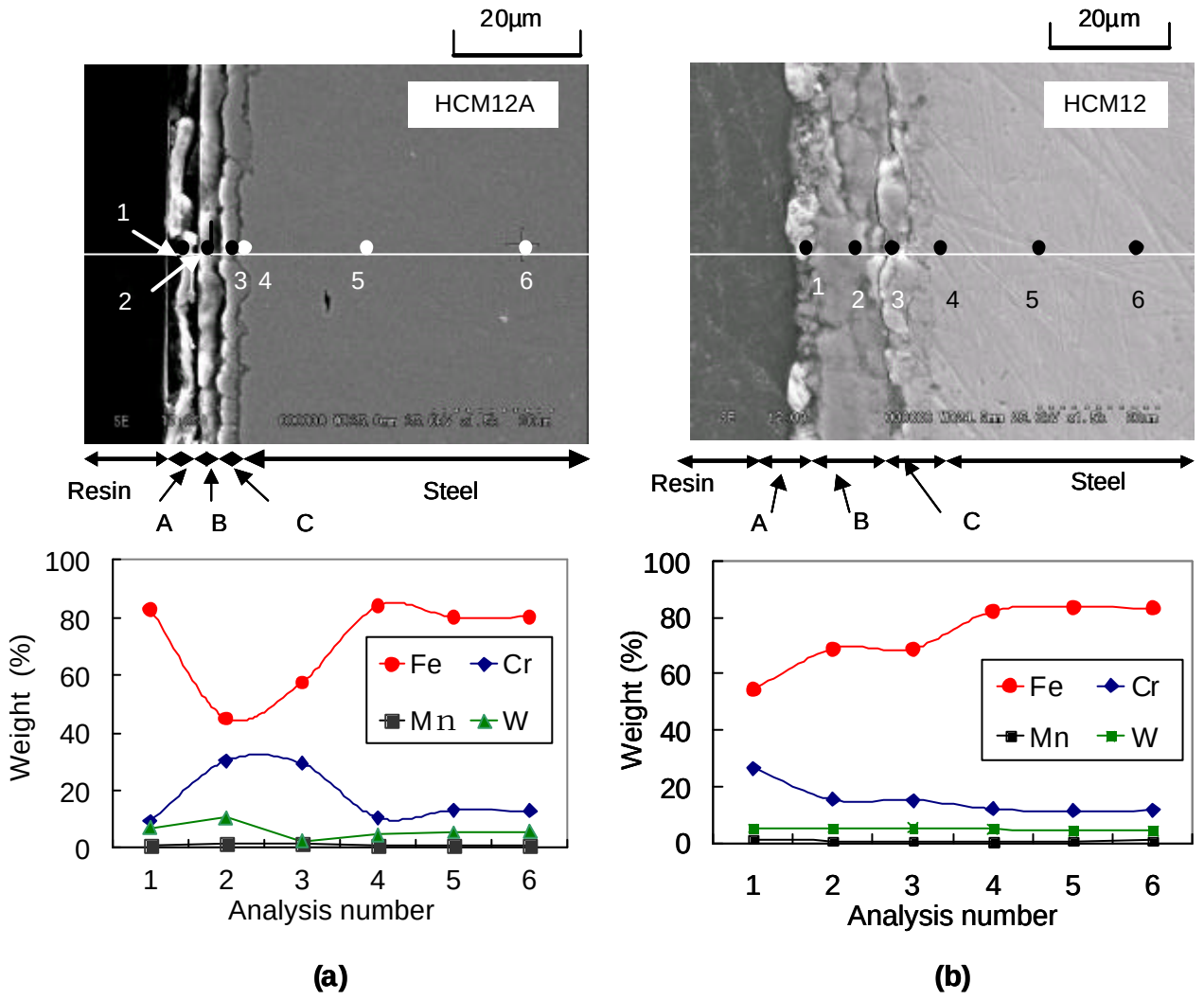

Fig. 7 Oxide layers and metal elements in (a) HCM12A and (b) HCM12 after 1,000-hr exposure to the Pb-Bi flow

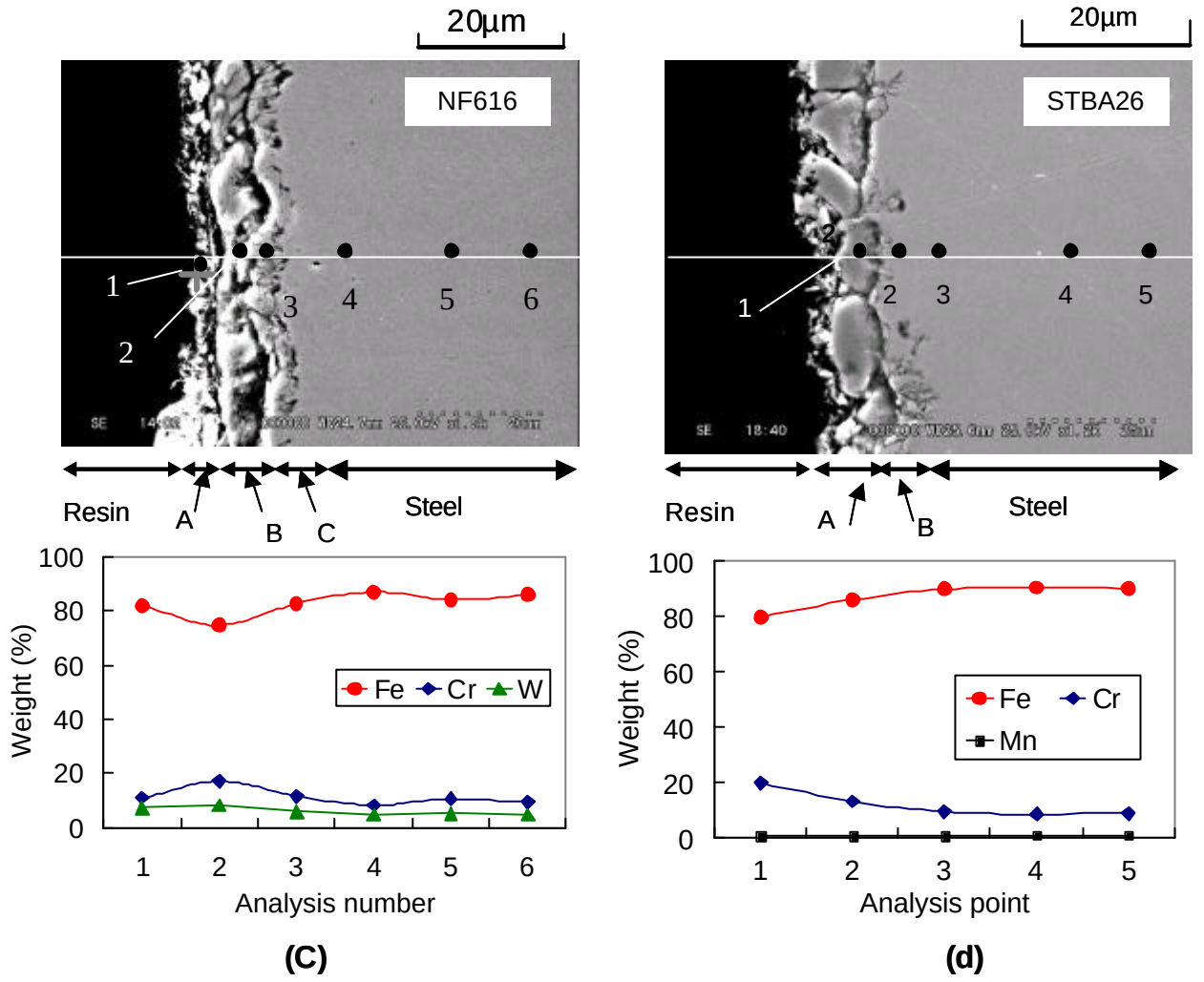

Fig. 7 Oxide layers and metal elements in (c) NF616 and (d) STBA26 after 1,000 hr-exposure to the Pb-Bi flow

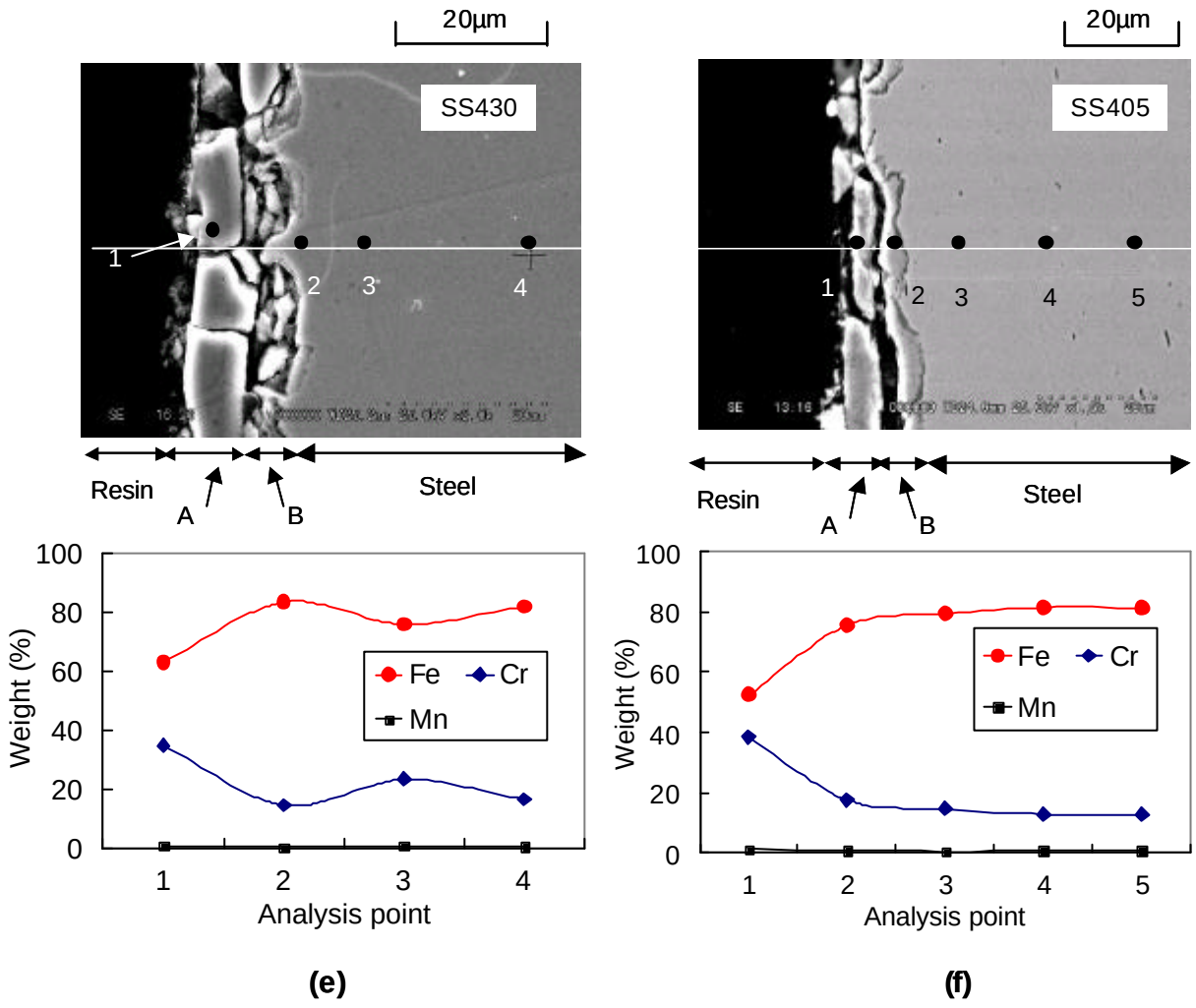

Fig. 7 Oxide layers and metal elements in (e) SS430 and (f) SS405 after 1,000 hr-exposure to the Pb-Bi flow

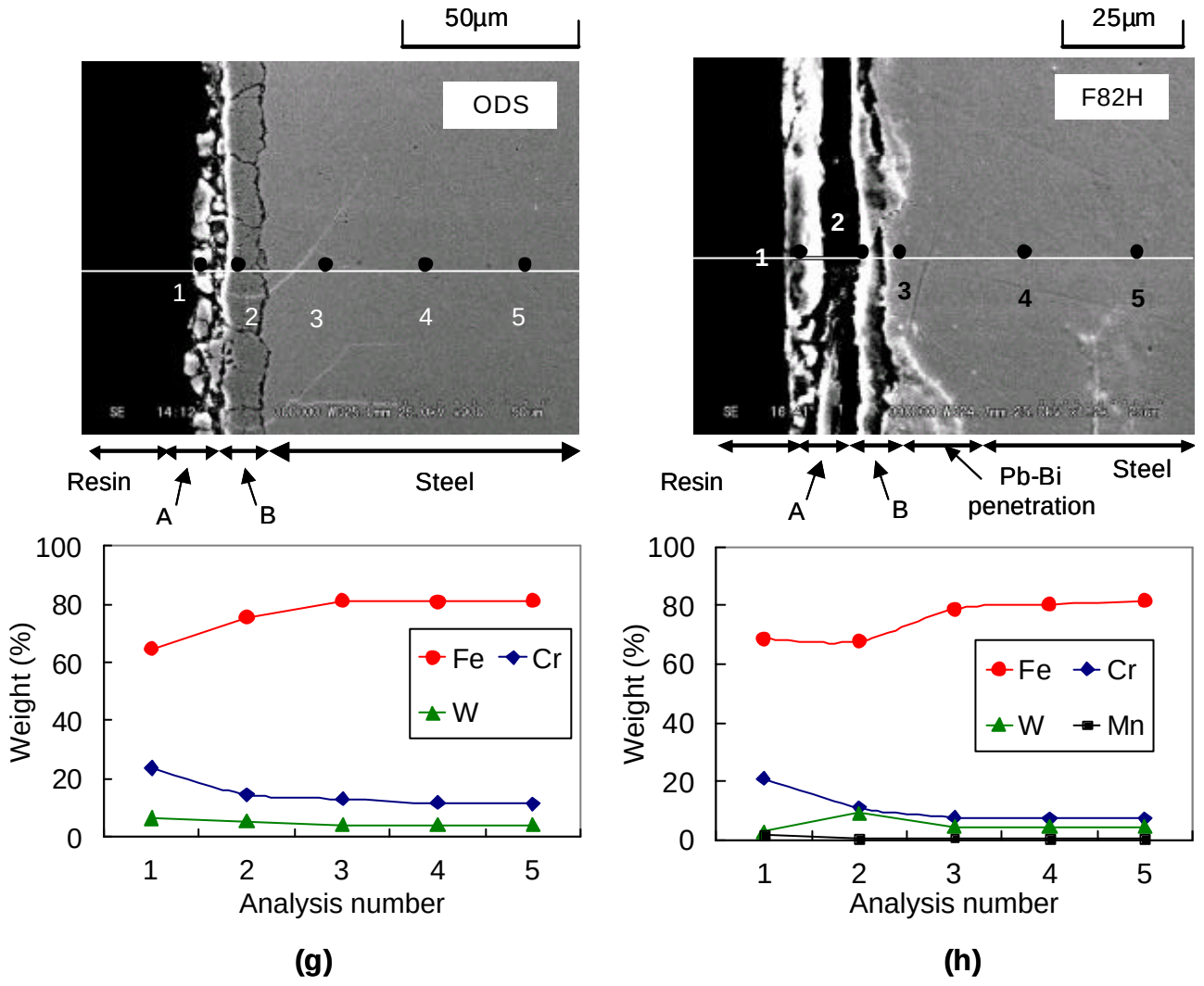

Fig. 7 Oxide layers and metal elements in (g) ODS and (h) F82H after 1,000 hr-exposure to the Pb-Bi flow

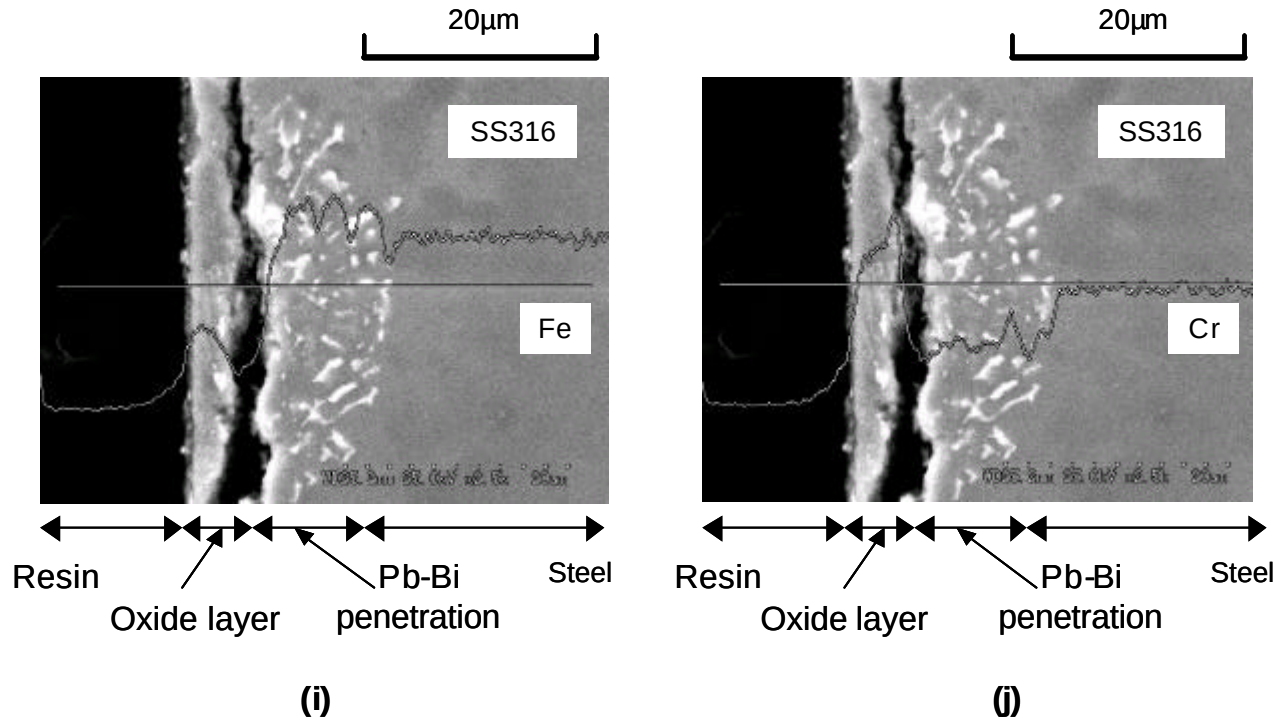

Fig. 7 Oxide layers and content of (i) Cr and (j) Fe in SS316 after 1,000 hr-exposure to the Pb-Bi flow

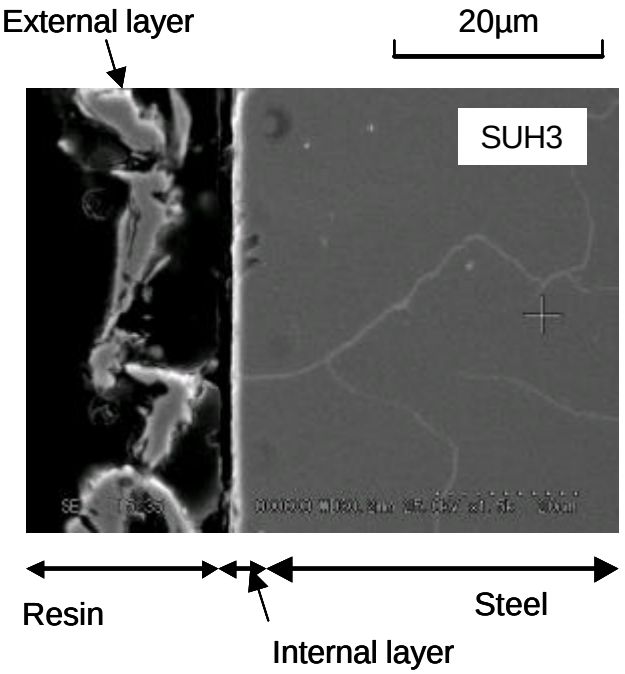

Fig. 7 (k) Oxide layers in cross section of SUH3 after 1,000 hr-exposure to the Pb-Bi flow

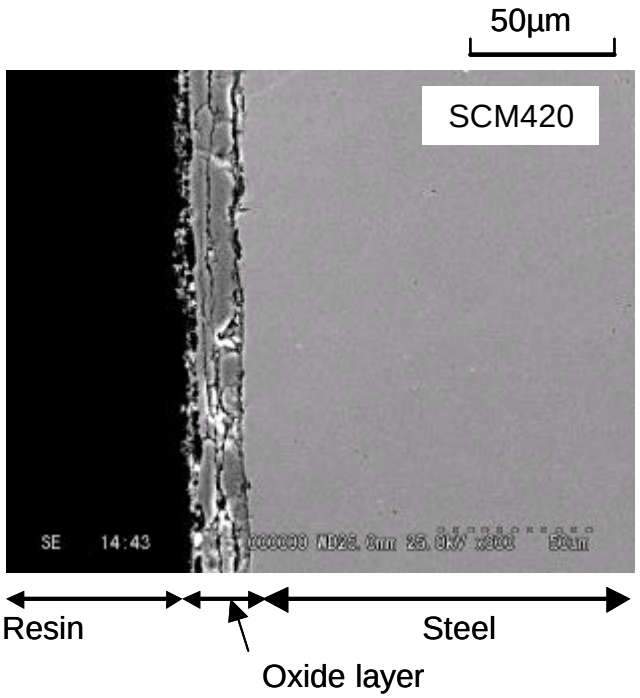

Fig. 7 (l) Oxide layers in cross section of SCM420 after 1,000 hr-exposure to the Pb-Bi flow

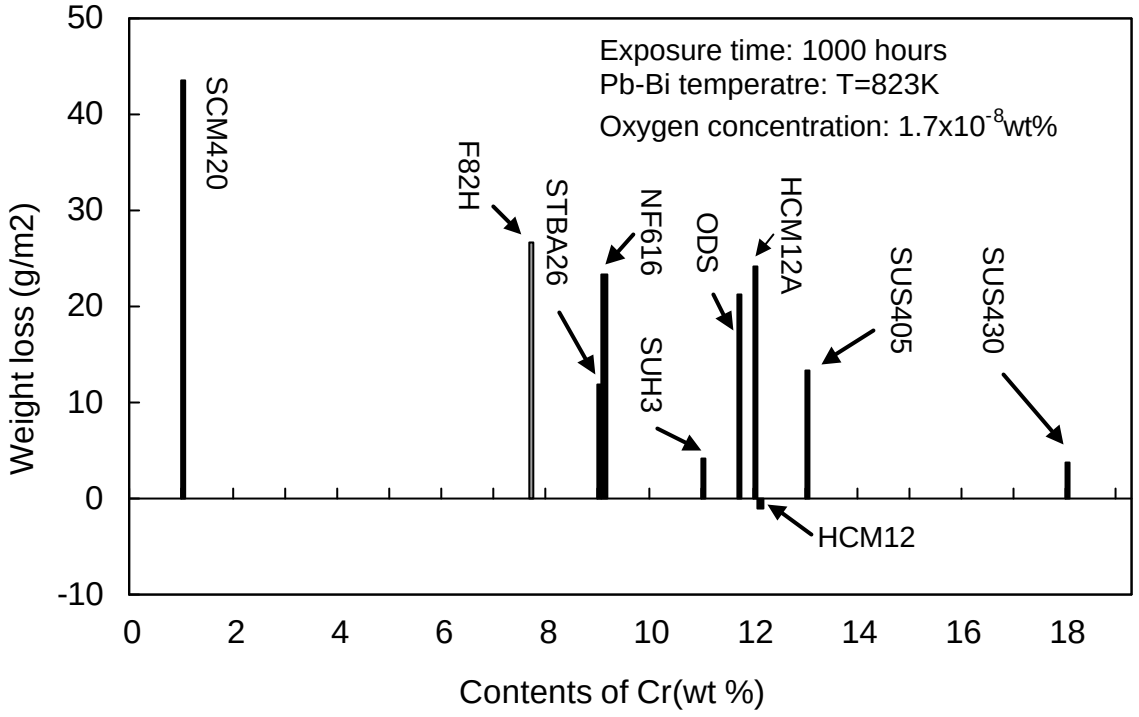

Fig. 8 Relation between weight losses and chromium content in steels